

DESIGN AND SIMULATION OF A BEARING HOUSING AEROSPACE COMPONENT FROM TITANIUM ALLOY (Ti6Al4V) FOR ADDITIVE MANUFACTURING

MOSES OYESOLA^a, KHUMBULANI MPOFU^a, ILESANMI DANIYAN^{a,*},
NTOMBI MATHE^b

^a Tshwane University of Technology, Department of Industrial Engineering, Staatsartillerie Road, Private Bag X680, Pretoria 0001, South Africa

^b National Laser Centre, Council for Scientific and Industrial Research, Laser Enabled Manufacturing, P. O. Box 395, Pretoria 0001, South Africa

* corresponding author: afolabiilesanmi@yahoo.com

ABSTRACT.

In evaluating emerging technology, such as additive manufacturing, it is important to analyse the impact of the manufacturing process on efficiency in an objective and quantifiable manner. This study deals with the design and simulation of a bearing housing made from titanium alloy (Ti6Al4V) using the selective laser melting (SLM) technique. The Finite Element Analysis (FEA) method was used for assessing the suitability of Ti6Al4V for aerospace application. The choice of Ti6Al4V is due to the comparative advantage of its strength-to-weight ratio. The implicit and explicit modules of the Abaqus software were employed for the non-linear and linear analyses of the component part. The results obtained revealed that the titanium alloy (Ti6Al4V) sufficiently meets the design, functional and service requirements of the bearing housing component produced for aerospace application. The designed bearing is suitable for a high speed and temperature application beyond 1900 K, while the maximum stress induced in the component during loading was 521 kPa. It is evident that the developed stresses do not result in a distortion or deformation of the material with yield strength in the region of 820 MPa. This work provides design data for the development of a bearing housing for AM under the technique of SLM using Ti6Al4V by reflecting the knowledge of the material behaviour under the operating conditions.

KEYWORDS: Additive manufacturing, bearing housing, FEA, titanium alloy.

1. INTRODUCTION

In evaluating emerging technology such as additive manufacturing, it is important to analyse the impact of the manufacturing process on efficiency in an objective and quantifiable manner. Over the years, several production methods, such as casting and conventional machining, have been used for the development of the high-value bearing housing component. However, the quest for efficiency in line with the Fourth Industrial Revolution (FIR) has brought about recent advancement in the use of additive manufacturing (AM), specifically the selective laser melting (SLM) process. Component simulations are very important in determining generic performances and can provide a comprehensive way to understand the behaviour of components or a material in service before the manufacturing process [1]. The process is usually iterative, thus, paving the way for adjustments of the process conditions in order to come up with the best component design that will meet the required service and functional requirements. This approach provides the required control right from the design phase in order to prevent expensive reworks. The use of titanium alloy is increasingly gaining widespread attention across the

fields of aerospace, medical, and automotive engineering, and many more, due to its excellent mechanical properties. In the field of aerospace, titanium alloy has been used for many years mostly due to its mechanical properties advantage [1–3]. Commercially, among the benefits that either titanium alloys or pure titanium offers as a material are high strength-to-weight ratio (density being 60 % of steel), light weight, and outstanding temperature strength [4]. Furthermore, Ti6Al4V is the most commonly used titanium alloy where high reliability is required due to its superior mechanical properties to others [4]. Similarly, the demand for titanium in manufacturing processes is growing with the target for sustainability of aircraft metal parts production owing to its environmental friendliness [5]. The properties of the titanium alloy depend on the microstructure, the size and arrangement of the alpha and beta ($\alpha + \beta$)-alloys phase where temperature is one of the factors that can significantly alter the microstructure coordination [6–8]. Hence, the quest for components supporting high-performing and light-weight bearings in aerospace applications require proper design, simulations and a good quality operation prediction control.

Bearings are components that find applications in the shaft of the aircraft engines, accessory gear box, landing gear, aircraft turbine, and numerous other places of use. Bearings used in any type of aerospace machinery must meet strict standards for material and quality control due to the harsh environments of operation. There are material standards, testing requirements, and required traceability on all parts. One of the characteristics required for bearings of a jet engine main shaft is the auxiliary power units for absorbing stress and providing support for loads [9]. The key characteristics required for the bearings in a jet engine main shaft are:

- suitability for high-speed rotation,
- high operating temperature,
- high reliability and traceability.

The main features of a bearing in its housing are in three forms, namely; bearing types (three-point contact ball or cylindrical roller), bearing material, and bearing design. Recent jet engines are designed to operate at higher temperatures and pressures for a lower fuel consumption, and to have a lighter weight [9]. These are key requirements in the quest for sustainability in terms of energy consumption and environmental friendliness as well as in the operational performance of the aircraft. The structure of the bearings for jet engine main shafts is becoming more complicated, hence reliability of the bearing housing must be improved. This important development task is being pursued on several fronts as in this study for AM [10]. To accommodate the wide variety of performance characteristics designs and manufactures, the development of bearing with a high reliability is necessary. The usual production methods of a bearing and its housing since ages-wise are through conventional machining and casting techniques [11]. The development of a bearing housing through the conventional means are met with some challenges, which can be suitably addressed with the use of AM technologies. For instance, the dynamics of service requirements necessitates the development of a bearing housing with improved quality. The improvement in the quality often requires some degree of flexibility during the design and manufacturing phase. Compared to the conventional methods, the AM technologies provide a high degree of flexibility tolerance during the product development. Furthermore, the Laser-Powder Bed Fusion (L-PBF) of Additive Manufacturing technology known as Selective Laser Melting (SLM) has gained an increased attention in recent years due to the ability of the process to produce near-net shape parts directly from CAD files without the retooling cost associated with casting or forging [11]. This makes the process considerable cost-and-time effective as compared to the conventional means. With SLM, traditional manufacturing processes, such as cutting, milling and grinding will not be necessary. Benefits include:

- (1.) new designs not possible using conventional subtractive technology,
- (2.) dramatic savings in time, materials, waste, energy and other costs of producing new components,
- (3.) significant reductions in environmental impact,
- (4.) faster time-to-market.

SLM builds up finished components from a raw material powder, layer by layer, through laser melting. Hence, the performance consideration of the process towards producing the referenced component of bearing housing directly.

The aircraft engine operates at very high temperatures, hence, a bearing part development must take into consideration the use of process that retains excellent mechanical properties at high temperatures such as the SLM. This is because a high temperature can promote cyclic stress and fatigue that can cause the bearing support to fail catastrophically in service. Furthermore, bearings developed for aircraft applications should be suitable for high speed rotation with excellent fracture strength to withstand the stress developed [12]. The desirable mechanical properties that must meet the required service conditions include; excellent wear resistance, hot-hardness, high strength-to-weight ratio [12]. While the design takes account of the suitable specifications for the required service conditions, the Finite Element Analysis (FEA) will examine the behaviour of the component as well as its mechanical properties under varying temperature. This will enable the manufacturer to ascertain the adequacy of the design for the required service conditions. To determine the effects of a varying dynamic response and excitation of components, a simulation model that includes specific geometric constraint assumptions needs to be developed. A simulation model of FEA that determines the dynamic response of the bearing housing component, which interpolates the solution from a set of precomputed values to provide faster results for design purpose, is required for a conformance investigation.

FEA is a powerful computer simulation tool, which has been adopted in many industries, including the aviation and automotive industry, for studying the behaviour of engineering systems under a variety of loading conditions. The reliability of a bearing housing is expected to be improved via proper design and FEA is a good quality control tool. This tool helps to determine manufacturability and heat treatment processes in order to ensure that the developed bearing component conforms to the standards. The FEA and simulation tools such as Abaqus has not only been valuable for maximising the performance of products, but also found useful applications in the development of more detailed instructions for operating and maintaining a finished component [10–12]. The SLM is one of AM technologies for metal fabrication with a processing capacity of good manufacturing accuracy and it is considered suitable for the purpose of this

work. This is because the process possesses an excellent controllability of internal complex structures for aerospace parts with large-scale and thin-walled complex structures [11].

Many works have been reported on the development of titanium alloy for aerospace applications. For instance, Zhu et al. [13] reported on the aerospace system and component design for light-weighting while Huda and Edi [14] reported on the material selection in the design of structures and engines of supersonic aircrafts. Inagaki et al. [15] reported that the use of titanium alloy for aerospace application has several merits, such as high compatibility with carbon fibre reinforced polymer, reduction in the maintenance cost, excellent fatigue strength and fracture toughness, high crack propagation, and good heat and corrosion resistance. Although the use of aluminium alloy brings about significant high strength-to-weight ratio of the aerospace component, it also has a drawback of reducing the strength of aluminium as temperature exceeds 200 °C [14, 15]. As such, aluminium alloy may fail catastrophically under the required service conditions, especially in extreme situations when the temperature exceeds the threshold. However, titanium is more suitable for high temperature applications though there is a need for the investigation of the thermal loads necessary for such service requirement because of its low thermal conductivity that can result in build-up stresses [16, 17]. The successful adoption of AM technology within the industry depends on its ability to reduce manufacturing costs and lead times without compromising the quality and mechanical properties of the finished product. In recent years, AM has had considerable successes in prototyping within the aerospace industry, permitting rapid design and product modifications, which in turn have enabled the final components to be manufactured quickly without a long lead time. In recent years, General Electric (GE) has been at the forefront of AM adoption for aircraft propulsion systems, integrating several AM technologies into new product developments. One landmark application of AM in the aerospace industry is the fabrication of individual fuel nozzles made of titanium to be used in a single commercial “Leading Edge Aviation Propulsion” (LEAP) engine by “Cubic Feet per Minute” (CFM) [18].

In terms of utilization in the aerospace industry, the primary PBF techniques comprise selective laser melting (SLM) and electron beam melting (EBM) [19]. The primary benefit of SLM and PBF, in general, is their ability to produce components of high resolution and quality, making their applications in the aerospace industry particularly useful.

In SLM, the build operation typically takes place in a vacuum or inert atmosphere (argon or nitrogen) to prevent the formation of surface oxides on the molten metal layers. The SLM process is very similar to direct metal laser sintering (DMLS) and SLS, with both undergoing a complete powder melting regime

The laser beam provides a sufficient energy to raise the powder above its melting temperature, creating a small region termed the ‘melt pool’ at an exact location that corresponds to the 2D projection of the CAD model. While SLS can utilise a range of polymers, metals, and alloy powders, and DMLS exclusively metals, SLM is primarily focused on particular metals, such as steel, aluminium, and titanium [19].

However, both DMLS and SLS lack the capability to fully melt the deposited powder material while the SLM has the ability to do so, resulting in the latter’s superior mechanical properties [20]. The primary benefit of SLM and PBF, in general, is its ability to produce components of high resolution and quality, making its applications in the aerospace industry particularly useful. In recent years, common metallic materials used to fabricate components for the aerospace industry have included tool steels and stainless steels, titanium, nickel, aluminium, and alloys of these materials [20]. Ti6Al4V alloy has gained widespread attention in the aerospace industry due to its combined properties of high strength, fracture toughness, and low density, together with a low coefficient of thermal expansion [21]. Significant efforts have been made in recent years to insert AM componentry into both structural and propulsion systems of aircrafts. Airbus used AM to produce A350 brackets from Ti6Al4V in 2014, the first metal AM components used for the interior of a commercial aircraft [21].

The objective of this paper is to perform the FEA of the bearing housing component from Ti6Al4V using the commercial software code Abaqus®.

The motivation for this work is the need to develop an aero-based component that will meet the required service and functional requirements taking into consideration all relevant effects for high speed applications. The work, therefore, employs a fast dynamic simulation model, for the investigation of the material behaviour under the thermo-mechanical loading conditions. Therefore, a minimal set of degrees of freedom, and analytical and physical motivated solutions were reviewed in this study. The novelty of this work lies in the investigation of the suitability of adopting titanium alloy for AM of a bearing housing for aerospace applications. The use of titanium alloy for aerospace application keeps emerging and has not been sufficiently highlighted in the existing literature about AM technology.

2. MATERIALS AND METHODOLOGY

The method essentially consists of assuming the piecewise continuous function for the solution by obtaining arbitrary parameters in a manner that reduces the error in the solutions. Here, the maximum yield strength in the component of the bearing housing was determined and the material was developed to a safe stress limit within the varying value of 800 to 1200 MPa. The maximum stress induced in the material should be less than allowable stress (yield stress and tensile stress)

in order to ensure a satisfactory performance in service without failure. The geometry-based modelling was employed for quick meshing of variants of the whole model and numerous sub-models. The scripting and other process automation techniques made the modelling and evaluation the results easier and faster, greatly simplifying the process of strength verification. The process of strength verification will enable the determination of the variations in the strength of the components vis-a-vis the service requirements under different operational and thermal loading conditions. This will provide an insight into the material behaviour and the point at which failure is imminent. One of the merits of the modelling and simulation tool is that such variations in the critical parameter of the designed component can be estimated numerically and compared with the mechanical properties of the material, thus, making the verification process relatively reliable. The considered component life cycle design is for a proprietary bearing housing component (M50-FC200) with the approach to achieving a longer service life if AM is employed for manufacturing of the part. The state of the art computational tool utilised for the analysis of titanium alloy – Ti6Al4V material response, is FEA. The simulation tool employed for the part design is Abaqus© software 2017 suite, the Abaqus/standard analysis tool in the complete Abaqus environment and Solidworks®. A sequence of design steps, tailored assessments of the material, is made to suitably evaluate the manufacturability requirements of the product. The part is developed in CAD model and uses FEA to obtain the bearing housing component (M50-FC200) design.

For an aerospace application aerospace, the LPBF technique considered in this study is the SLM. The primary benefit of SLM is its ability to produce components of high resolution and quality, making its application in the aerospace industry particularly useful [7–10]. The use of SLM, being a technique of LPBF, assures the production of fully dense parts with high-quality and near-net shape. Therefore, it is perfectly suitable to meet strict requirements of the high-strength titanium alloys used in the aerospace; as examined in this study. The choice of Ti6Al4V stems from its high strength-to-weight ratio and excellent resistance to corrosion (in aqueous solutions, oxidizing acids, chlorides, rocket propellants and alkalis). It also resists to creep, remains strong and fracture-tough. This makes it a suitable candidate material for aerospace applications [22–24].

The implementation of near- β titanium alloys in a commercial aircraft, namely, Ti-10-2-3, Ti-15-3-3-3, and VT 22 (Ti-5Al-5V-5Mo-1Cr-1Fe, Ti-6Al-4V), which are all still used in the aerospace today, has been reported. In particular, Ti-10-2-3 has proved to be one of the most forgeable β -titanium alloys (low flow stresses), and it also exhibits a high resistance to edge cracking [25–27]. However, the strength-to-weight ratio of Ti6Al4V, coupled with its forgeability

and high resistance to edge cracking, are strong advantages of the material vis-à-vis the aerospace requirements. These characteristics enable significant time-reductions between reheats, reduce labour-intensive conditioning operations, increase materials yield, improve efficiency, and lower processing costs.

The simulation performance in this study is benchmarked against characteristics of strain rates, which occur over a wide range of Ti-alloys in commercial aircraft applications [25–27].

The comprehensive FEA simulation performed for the Ti6Al4V in this study provides a mechanistic basis for reliable applications of additively manufactured bearing-housing component. In the event of any pores developing during the production, the pores can be eliminated by using defects-free raw materials, optimising the processing parameters, and implementing a suitable post-processing treatment.

The chemical composition corresponding to ISO 5832-3 as well as the mechanical and electrical properties of the titanium alloy (Ti-6Al-4V) are presented in Tables 1 and 2, respectively.

Element	Al	Fe	O	Ti	V
Percent weight [wt %]	6	0.25	0.2	90	4

TABLE 1. Chemical composition of titanium alloy (Ti-6Al-4V) [28].

S/N	Properties	Value
Mechanical		
1.	Yield strength	880 MPa
2.	Ultimate tensile strength	950 MPa
3.	Bulk modulus	150 GPa
4.	Modulus of elasticity	113.8 GPa
5.	Shear strength	550 MPa
Electrical		
1.	Specific heat capacity	553 J/kg K
2.	Thermal conductivity	7.1 W/m K
3.	Melting point	1878 K
4.	Coefficient of thermal expansion	$8.7 \times 10^{-6} \text{ K}^{-1}$

TABLE 2. Thermo-mechanical and electrical properties of titanium alloy (Ti-6Al-4V) [28].

Theoretical and numerical FEA models were then constructed and compared to the experimentally acquired data to assess the validity of the models and their efficacy in predicting the thermal behaviour of the designed component. The design considerations include the suitability for high speed and temperature application as well as high strength to support the load and absorb the induced stress [17]. The bearing was subjected to a working temperature ranging

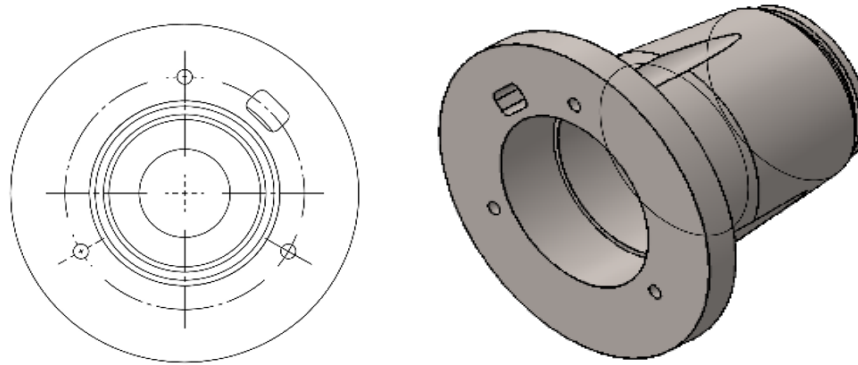


FIGURE 1. The 3D CAD models generated for the bearing housing.

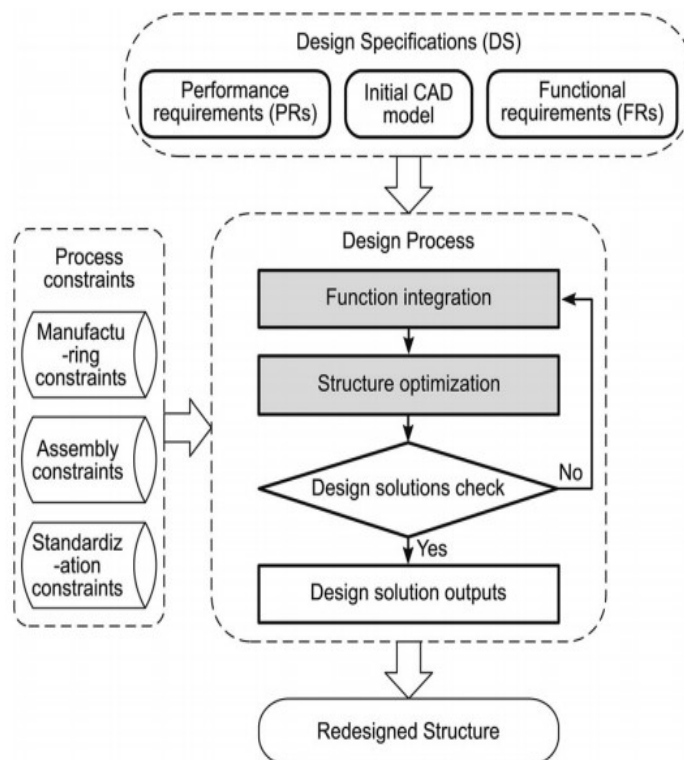


FIGURE 2. AM-enabled design method proposed by Yang and Zhao [29].

between 573.15–623.15 K. This is because the bearings of the aircraft engine main shafts are exposed to a temperature of approximately 473.15 K during the operation. The turbine remains in the heat soak retaining heat without any escape even after the engine stops, thereby raising the bearing temperature to over 573.15 K. Hence, the modelling and simulation package of the Abaqus is employed to study the stress and temperature distribution of the bearing in order to determine its mechanical behaviour under high temperatures. The modelling process starts with the generation of 3D CAD models that accurately mimic the components to be studied (Figure 2).

In assessing the suitability of a product idea for production in AM, usually, a mapping of data between materials and process, geometrical structure and behavioural properties, is carried out in order

to ensure a better manufacturing. Likewise, a CAD model in Design for Manufacture (DfAM), which is particularly used for the design plan, is introduced in this section as the hypothetical case of the bearing housing component. The parametric CAD model of the mentioned bearing housing is developed and used in determining the functionality based on the part in the software package of Abaqus FEA. Firstly, the four main parameters of flexural bearing housing geometry were identified, these include the outer diameter, and the thickness according to the dictates of the technical drawing for the component. The CAD model is developed from a proprietary technical chart (M50-FC200) of aircraft application using Solidworks® as shown in Figure 1.

The Von Mises stress analysis was used as the failure criterion during the finite element analysis carried

out with the aid of the modelling and simulation tool (Abaqus). The failure of the material occurs at a point in a member when the distortion strain energy in a bi-axial stress system reaches the limiting distortion energy. At this point, the material starts yielding to further application of load. The maximum distortion energy for yielding is expressed as Equation (1):

$$(\sigma t_1)^2 + (\sigma t_2)^2 - 2\sigma t_1 \times \sigma t_2 = \left(\frac{\sigma y_t}{\text{F.S.}}\right)^2, \quad (1)$$

where: σt_1 is the maximum principal stress (N m^2), σt_2 is the minimum principal stress (N/m^2), σy_t is the stress at yield point (N/m^2) and F.S. is the factor of safety.

In order to investigate the suitability of production based on Laser Melting of AM, a simulation was conducted using the aggregated parameters in Tables 1 and 2. The version of the Abaqus for the modelling and simulation was employed for the titanium alloy and the bearing housing model. The objectives for the simulation approach are to reduce and complement exhaustive pre-study experiments and costs implication. Given the physical and analytical structural dynamics modelling in this study, the mathematical models are further expressed using governing equations. To denote the arbitrary reference point for the mechanical-to-thermal field coupling in the SLM [11], the thermal transfer at material point r , determined in Lagrangian domain, is denoted in Equation (2):

$$\rho \frac{dH(r, t)}{dt} = -\nabla \cdot q(r, t), \quad r \in \Omega, \quad (2)$$

where ρ is the material density (kg/m^3), H is the enthalpy (J), t is time (s), q is the heat flux vector (W/m^2) and q is the volumetric heat input (J/K/m^3). Assuming a linear dependence of the heat flux on the temperature gradient, i.e., Fourier's law, the heat flux vector can be determined from Equation (3):

$$q = -k(T) \nabla T(r, t), \quad (3)$$

where k is the thermal conductivity ($\text{W/m}^\circ\text{C}$), assumed to be isotropic, T is the temperature (K). The temporal rate of enthalpy can be written as Equation (4):

$$\frac{dH(r, t)}{dt} = C_p(T) \frac{dT(r, t)}{dt}, \quad (4)$$

where C_p is the specific heat (J/g K). The volumetric heat input q in Equation (2) is the heat energy input, which plays a key role in the determination of the amount of heat needed to cause melting of the starting powders in the SLM process modelling. The meshing of the bearing housing at different orientations in order to predict the material's behaviour are described in the Results and discussion section.

2.1. MANUFACTURABILITY ANALYSIS AND AM DESIGN RULES

AM design rule collections ensuring manufacturability and approaches related to AM design potentials for development of innovative solutions must be taken into account. While AM provides huge design potentials, geometric freedom is not unlimited. In the literature, design rule catalogues can be found particularly for SLM. The geometric limits imposed by SLM are based on series of experiments and design for manufacturing. Munguia et al. [30] use an advice system based on artificial intelligence to compare additive and conventional manufacturing in order to recommend optimal production parameters. The second category aims at choosing an optimal production strategy depending on product requirements and process limitations.

Depending on manufacturability indexes calculated by design parameters, a CAD model is divided into a modular structure whose parts are manufactured separately and which are then assembled. Due to the novelty of AM for designers and producers, the selection of appropriate candidates remains a challenge. Figure 2 presents the AM-enabled design method proposed by Yang and Zhao [29]. The design method presents the basic process constraints, which encompass the manufacturing, assembly and standardisation constraints as pre-conditions for the process design. These constraints are integrated into the design process loop as presented in the Figure 2. The framework identifies the performance and functional requirements as two critical requirements that should be addressed by the process design. The functional integration can be achieved via the structural optimisation and the process is looped until the required design solution is obtained. The computer-aided modelling and simulation approach is often suitable for a performance evaluation of the designed solution (solution check) before proceeding to the final stage of manufacturing. This is because the approach is iterative and often allows the structural optimisation and adjustment of the design parameters and constraints until the final solution converges and the desired requirements are met. In addition, the modelling and simulation of the designed solution at this stage will promote the overall cost and time effectiveness of the overall process, thereby bringing about the development of components with high integrity without the need for expensive reworks. The designed solution output can also be compared with the ideal solution in order to estimate the design error and its level of permissibility.

Concurrent engineering has been a useful methodology that takes into account the attributes of each different stages of product's life cycle simultaneously. It is used to integrate all activities of functional analysis and requirement engineering, design, and manufacturing in parallel during the design stage as an integrated design. Several authors have reported on the difficulties in getting a Laser Powder Bed Fusion part of SLM when the dimensions are large (280 mm by 280 mm).

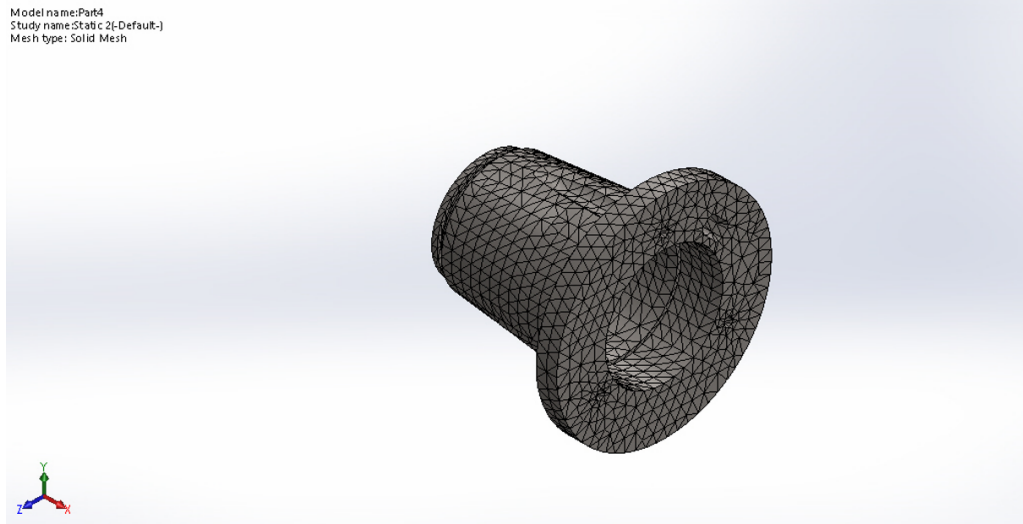


FIGURE 3. Component solid mesh.

This is because cracks usually occur due to internal stresses and this accounts for the reason why a lot of post-processing is needed to avoid cracking, like stress relieving and hot isostatic pressing [31].

The mathematical formulation of variables for the bearing housing orientation angles and layer thickness is expressed in Equation (5):

$$x = \{\theta_x, \theta_y, \theta_z, L_t\}, \quad (5)$$

where: $\theta_x, \theta_y, \theta_z$ signifies the part orientation with respect to angles between the part in x , y , and z axes. The angles show the orientation of the part in the build area while L_t is the layer thickness required during fabrication, the layer thickness value is between L_t min and L_t max.

2.2. THE FINITE ELEMENT ANALYSIS

Finite Element Analysis (FEA) is a method based on homogenised pictures, employed to better understand the underlying consolidation part of product development. The method consists of assuming the piecewise continuous function for the solution and deploying the parameters of the functions in a manner that reduces errors in the solution. The simulation of the Ti-6Al-4V alloy bearing housing as mentioned was, therefore, carried out. The maximum stresses were assigned to an allowable stress of component material to obtain maximum stress design for the bearing housing.

The FEA and simulation serves to provide a precursory visualisation of the response of the developed component during its eventual commissioning for in-service operations. The simulation was carried out using operating parameters representing extreme service conditions in order to obtain some knowledge on the limits of its mechanical integrity.

The implicit module of the Abaqus software was employed for the non-linear analysis of the component part. This is because the implicit dynamic simulations can be applied to component analyses, which

are non-linear in nature. The explicit module has a suitable integrator for the formulation and analysis of a non-linear behaviour. It is an iterative process and the time increment is adjusted until the solution converges. Following the meshing of the assembly into finite elements, it was subjected to convergence simulation runs with mesh refinement feature employed for the ease of convergence. An average mesh size of 0.8 mm, which falls within the seed size stability convergence zone, was employed for cost and time efficiency. One of the assumptions is that the loading is static and that the material is subjected to the same different loading and service requirements in all its parts. A structured 8-node hexahedral mesh element type with a linear displacement and temperature advancing front using Abaqus was employed. This was selected to mesh the assembly into finite elements, and thereafter subjected to convergence simulation runs with the mesh refinement feature employed for the ease of convergence.

2.3. MESH GENERATION AND GEOMETRIC MODEL

The mesh generation and geometric model was performed using Solidworks tool to maintain computational accuracy and convergence check balance. The mesh elements parameters were carried out at the joints. The convergence check gave an indication of suitability of 2 mm as the optimum mesh geometric model. A four-node thermally-coupled tetrahedron linear displacement standard solid mesh is employed in discretising the model into finite elements. A mesh size of 2 mm is used for the analysis from node to node over the entire geometry of the model in Figure 3.

For the convergence range, an average mesh size of 2 mm, which falls within the seed size stability convergence zone, was employed, in order to strike the right balance among the computational efficiency

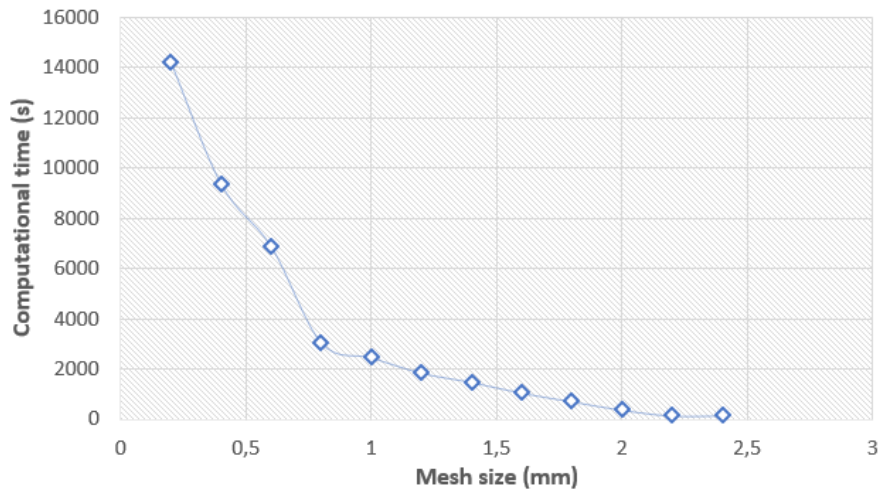


FIGURE 4. Mesh size and computational time.

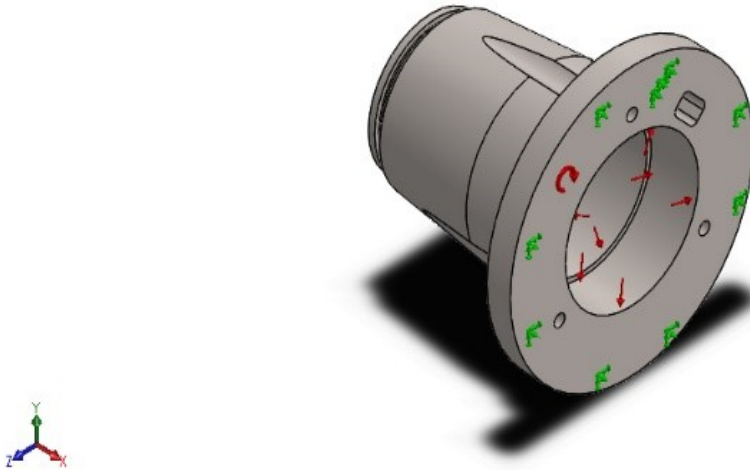


FIGURE 5. Model of the bearing housing.

and accuracy in contrast with other mesh sizes within the convergence band.

The mesh, element sizes and the convergence in the results between mesh sizes 1.8 mm and 2.4 mm indicates that any mesh size within this convergence range provides the best confidence in accuracy of the simulation result. Thus, a 2 mm mesh size was selected owing to the fact that it provided the least amount of computation time, which is very important, as time is a key factor in computer aided design and manufacturing.

The mesh size plays a vital role in the accuracy of results and computing time as it determines the number of elements involved. On this note, the computational time against the mesh size is presented using a mesh interval of 0.2 mm as presented in Figure 4. It was observed that the computational time decreases with an increase in the mesh size up to 2.2 mm. Further increase in the mesh size up to 2.4 mm resulted in

a slight increase in the computational time. Hence, the mesh size of 2.2 mm, which produced the least computational time (142 s), was selected. Figure 5 presents the model of the bearing housing.

The component is further analysed in Solidworks and assigned temperature-dependent material properties for elasticity, plasticity, and thermal response, with Ti-6Al-4V alloy selected from the material database. The guidelines for the bearings for jet engines were considered for the identification of the product's properties in relation to the service requirements [32]. The emphasis on the Ti-6Al-4V alloy is due to its main features, which are light weight, high strength (yield strength of approximately 1000 MPa), high temperature characteristics (maximum melting point for grade 5 is at 1933 K), thermal processability, fracture toughness, workability, and superior formability [33–36]. This alloy is currently the most preferred for aircraft manufacturing owing to its theo-

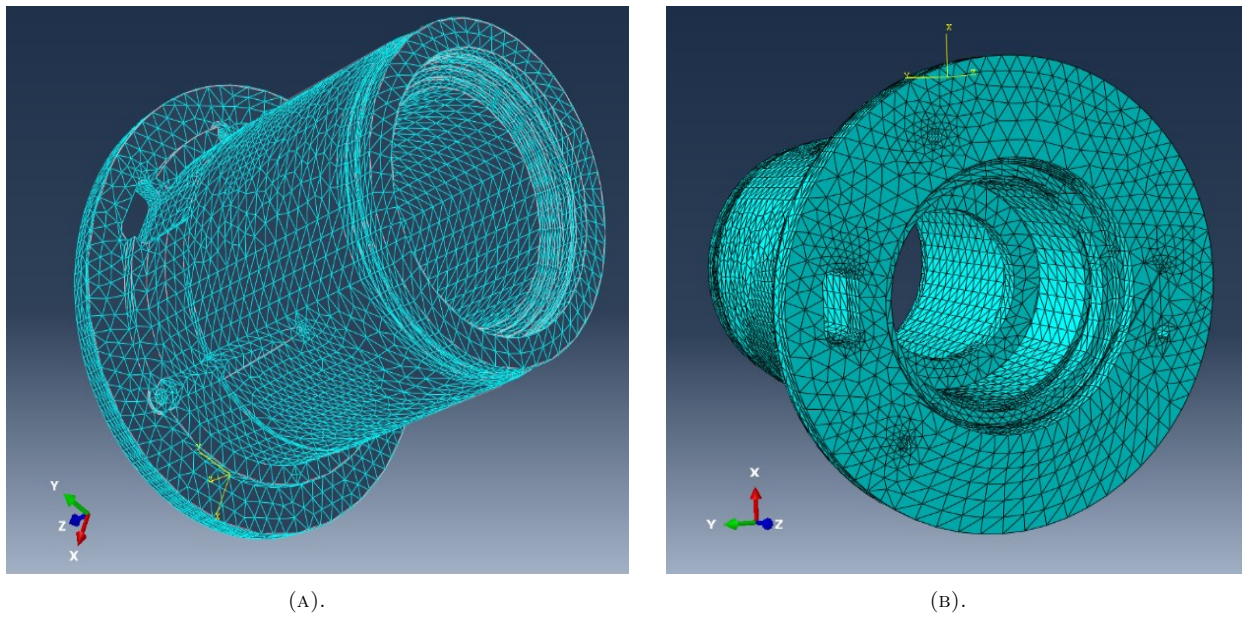


FIGURE 6. Component's mesh-based geometry as in FEA-Abaqus. (a) wireframe and (b) solid mesh.

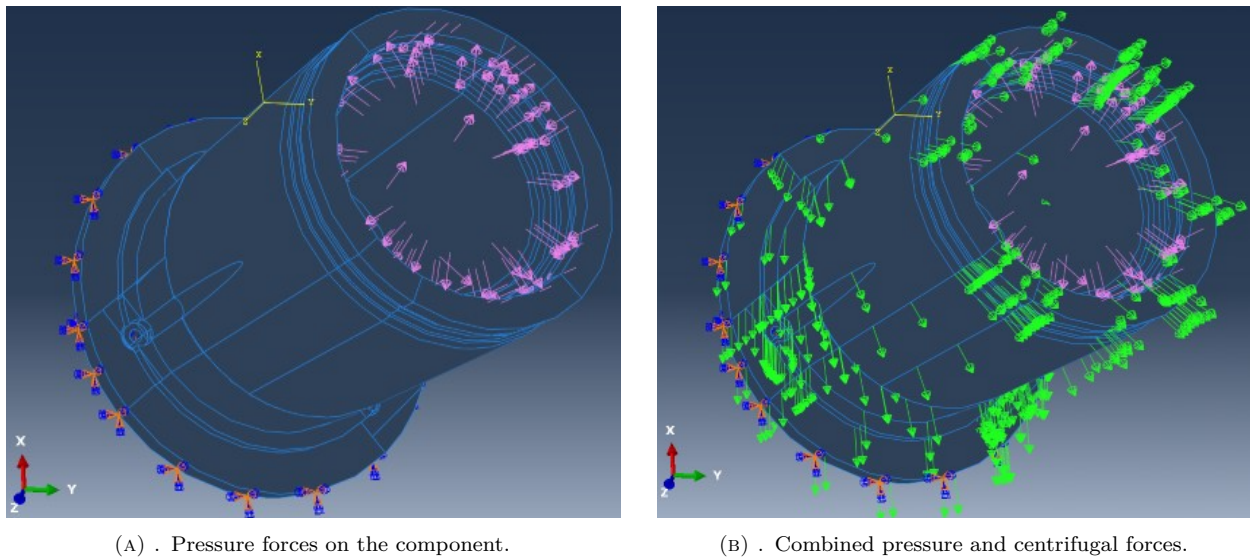


FIGURE 7. Visual mechanism acting on the bearing housing in Abaqus (a) and b).

retical chemical composition properties, good high-temperature properties and high strength-to-weight ratio [37, 38]. In addition, the availability of quantifiable data further increases its application for where the yield strength of annealed material is 825 MPa or higher, tensile strength is 895 MPa or higher, and elongation is 10% or higher at a room temperature [39].

The implicit module has a suitable integrator for the formulation and analysis of a non-linear behaviour as it is an iterative process with time increment adjustments until the solution finally converges. Following the meshing of the assembly into finite elements, it was subjected to convergence simulation runs with mesh refinement feature employed for the ease of convergence. Figure 6 present the component's mesh-based geometry as displayed in FEA-Abaqus.

2.4. PRESSURE AND CENTRIFUGAL LOADING CONDITIONS

In the operation of a typical aircraft-jet turbine engine, air is usually sucked in large volumes and compressed in the magnitudes of tons of air per second with the aid of fan and compressor in a coupled mechanism. The loads and fixtures used in the model, modelled in Solidworks, are presented in Table 3. While Figure 7 further illustrate the pressure and centrifugal forces acting on the component, modelled in Abaqus.

This understanding and philosophy of load often accounts for the centrifugal (green arrows) and pressure forces (purple arrows) acting on the components and the visual mechanism for the bearing housing is displayed in Figure 7.

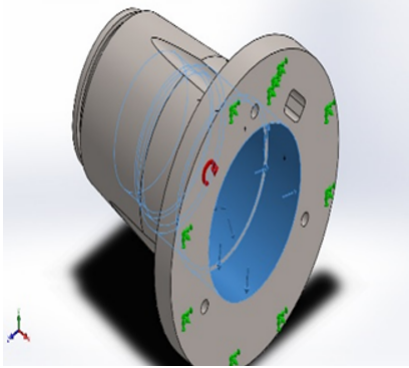
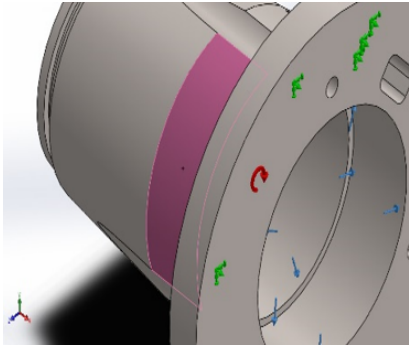
Load name	Load image	Load details
Pressure		Entities: 4 face(s) Type: Normal to selected face Value: 101 325 Units: N/m ² Phase angle: 0 Units: Deg
Centrifugal		Centrifugal, Ref: Face<1> Angular velocity: 1800 rad/s Angular acceleration: 0 rad/s ²

TABLE 3. Loads for pressure and centrifugal condition in Solidworks.

2.5. THERMAL BOUNDARY CONDITIONS

Aside from the philosophy of drawing air into the engine, the compressor also pressurizes the air, at ratios up to 40:1. This pressurised air is then delivered into the combustion chamber where it is ignited after the addition of fuel [40]. Hence, typical temperatures during this process may rise as high as 2273 K, thus accounting for the thermal stresses on components within and around the engine is critical. Typical ambient temperatures within the compressor ranges between 473 K and 1000 K [41] for the low-temperature creep behaviour of titanium. The thermal interaction for the bearing housing was further examined in Abaqus (Figure 8).

Thermal interactions were assigned to the model with the upper and lower bounds of 1973 K and 273 K, respectively, assigned as thermal boundary conditions in relation to the temperature bounds that can be experienced within the environment of the component during operation. Where the continuous flow of air or gases to which it is exposed may range from 1120 K to 1973 K. The higher temperature of 1973 K was used in the thermal analysis of the effects of convected temperature on the material as a worst-case operation scenario.

In the static general analysis, encastre boundary conditions in which all translational and rotatory motions are set at zero were assigned at the cap of the housing where it is often bolted to other components (as in Figure 8). Pressure loads of 101.325 kPa, the

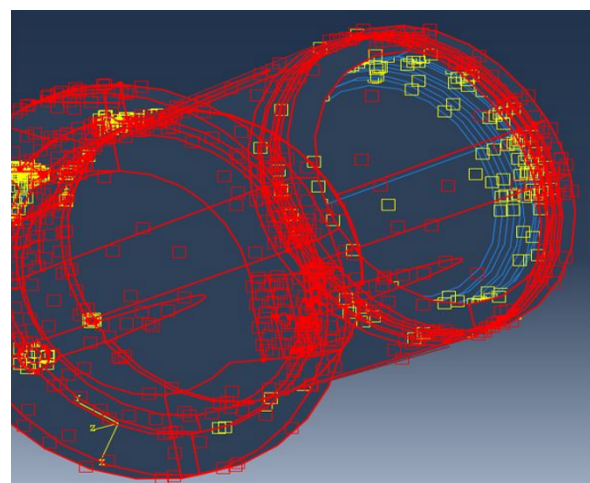
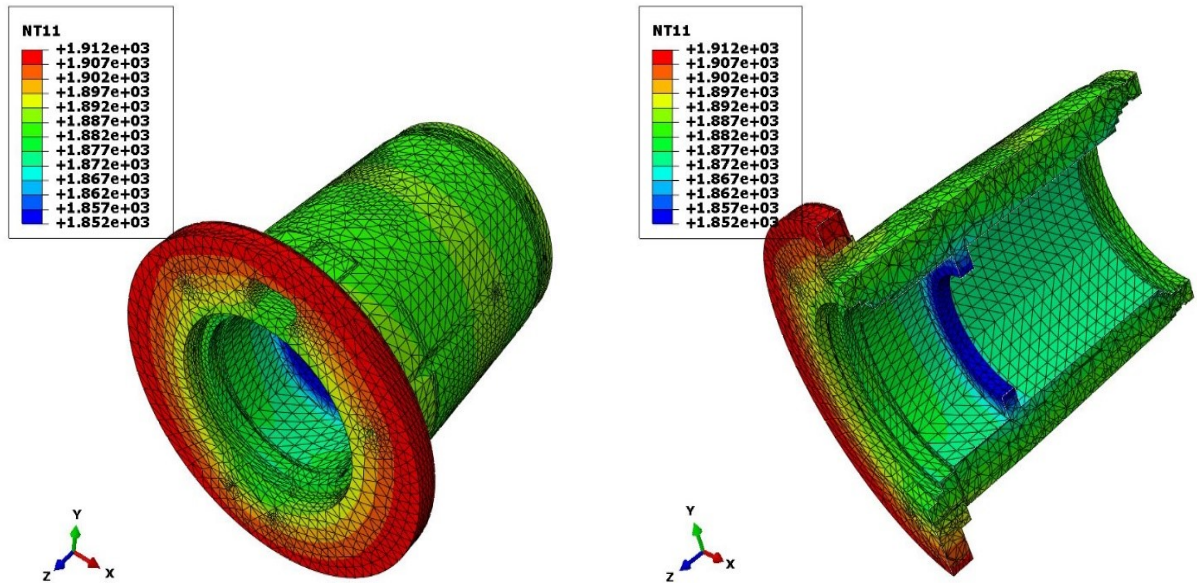


FIGURE 8. Thermal interactions for the bearing housing component.

atmospheric pressure of air at sea level, and arbitrary centrifugal load of 1800 rad/s were applied.

3. RESULTS AND DISCUSSION

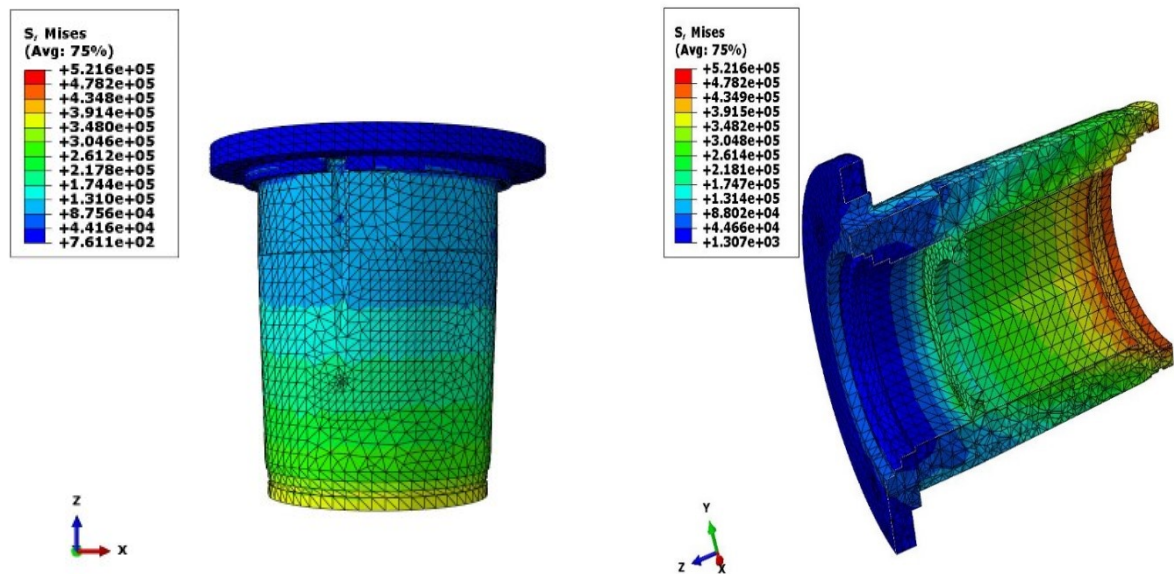
The results obtained for the Abaqus-FEA simulation are presented in Figures 9–13. The temperature distribution profile presented in Figure 9 shows the variation in temperature across the geometry of the component. The highest temperature achieved under the earlier stated thermal conditions is above 1900 K and was recorded at the periphery of the cap. A larger part of



(A) . Temperature distribution across the whole component geometry.

(B) . Temperature distribution – bilateral view of the component.

FIGURE 9. Temperature distribution on the bearing housing.



(A) . Superimposed stress distribution of thermal and pressure loading on the component.

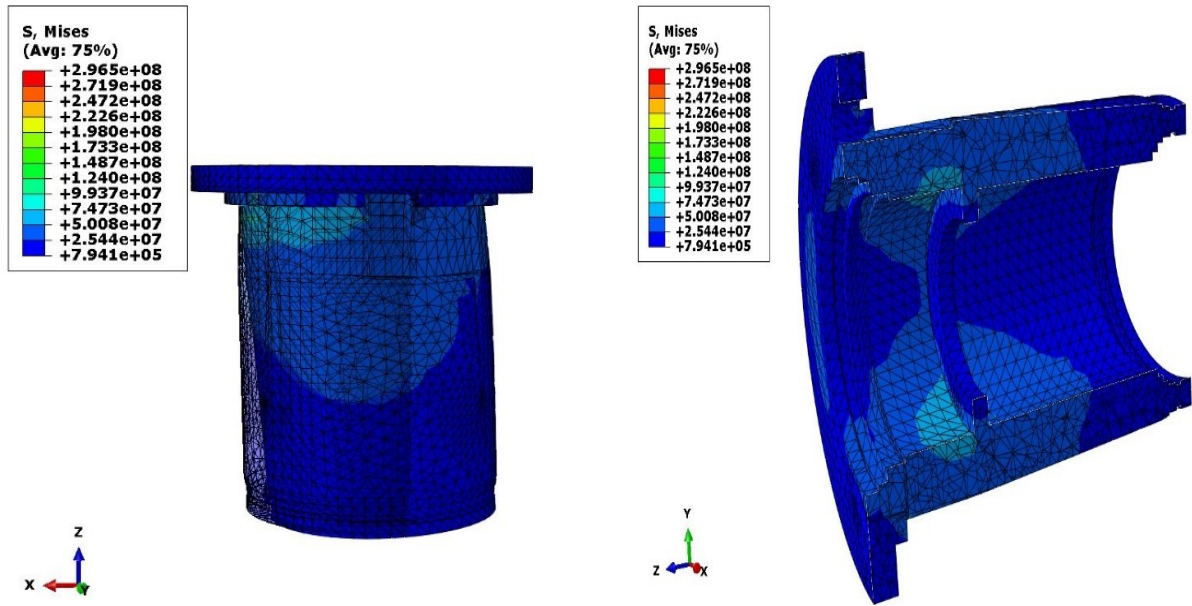
(B) . Superimposed stress distribution of thermal and pressure loading on the bilateral component.

FIGURE 10. Superimposed distribution of thermal and pressure loading.

the component does not heat up beyond 1900 K, which gives a strong indication of its ability to withstand such extreme conditions without melting, given the melting temperature of the material is about 1933 K. Figure 9 shows the temperature distribution during a steady-state operation.

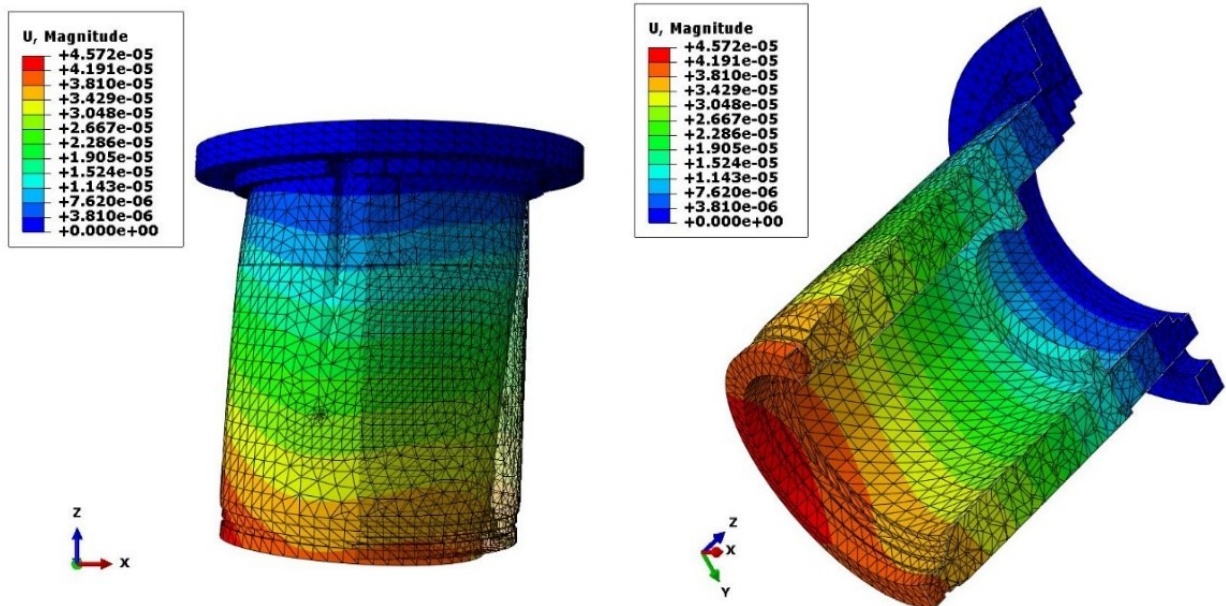
The response of the component to external forces and loading conditions is further presented. The effects of the mechanical loading regimes have been compared to investigate the material’s responses to the applied forces. Both the Von Mises stress profile

within the part and the magnitude do not pose any threats to the life or performance of the material under the reference operating conditions. Figure 10 shows the stresses developed due to air flow pressures and heat transfer, which are within a kilopascal range with the maximum Von Mises stresses being about 521 kPa. It is evident that the stresses developed do not result in a distortion or deformation of a material with yield strength in the region of 820 MPa. Figure 10 is the superimposed deformed or undeformed stress distri-



(A) . Superimposed stress distribution of thermal, pressure and centrifugal loading on the component. (B) . Superimposed stress distribution of thermal, pressure and centrifugal loading on the bilateral component.

FIGURE 11. Superimposed deformed/undeformed stress distribution.



(A) . Superimposed displacement due to thermal, pressure, and centrifugal loading on the component. (B) . Superimposed displacement due to thermal, pressure, and centrifugal loading on component bilateral.

FIGURE 12. Superimposed deformed/undeformed displacement due to coupled thermal, pressure and centrifugal loading.

bution due to coupled thermal and pressure loading only.

Remarkably, the contribution of centrifugal forces was found to be of significant magnitude as presented in Figure 11, as evidenced by its ability to raise the Von Mises stress three (3) orders higher than when they are suppressed. In addition, Von Mises stresses up to about 300 MPa are obtainable, which indicates that components experience some deformation. This is largely due to the torsional moments associated with

the centrifugal forces applied on the part. The superimposed deformed or undeformed stress distribution due to the coupled thermal, pressure and centrifugal loading is presented in Figure 11.

The displacements due to the deformation are presented in Figure 12, where the maximum displacement of 0.0457 mm is recorded at the free end of the part. This implies that the displacement due to the deformation is minimal.

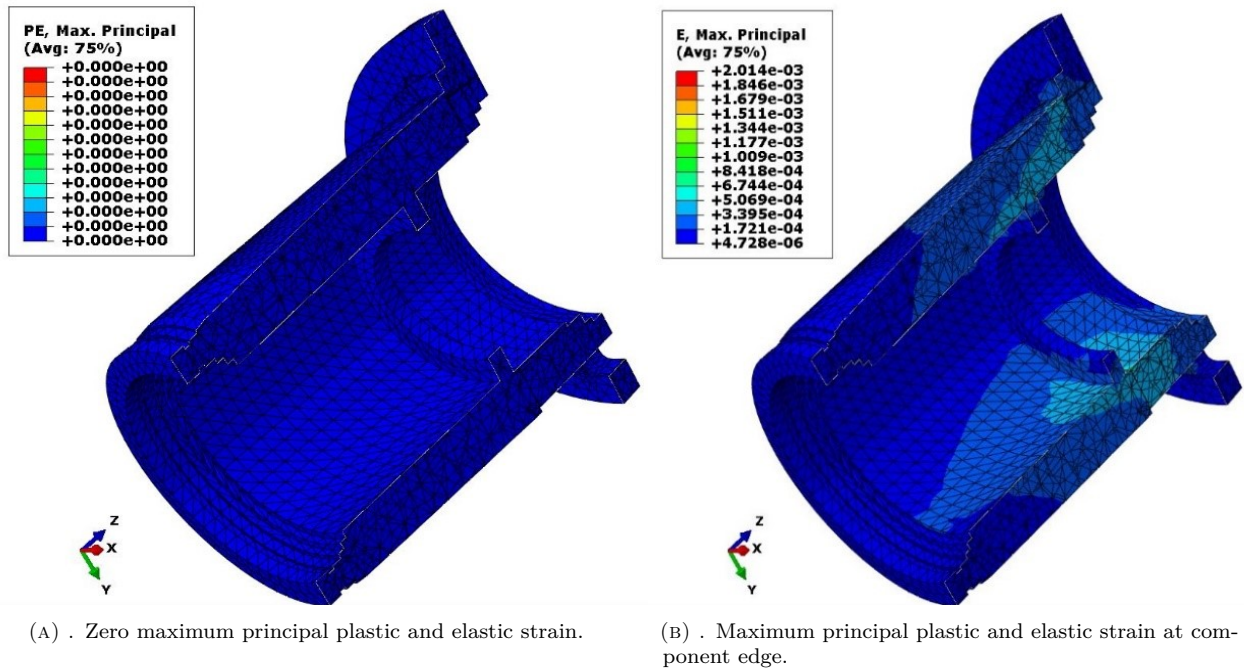


FIGURE 13. Maximum principal plastic and elastic strains due to coupled thermal, pressure and centrifugal loading.

Results, as shown in Figure 12, indicate the different aggregation of loads that may cause a slight displacement with magnitudes of the deformation attributable to the centrifugal loading regime imposed on the component while in service. Inferably, higher magnitudes of imposed loads than the ones considered could hypothetically amount to pushing the component's integrity beyond safe limits. Just like in every engineering material, loads that will push stress levels of the component beyond its yield strength of 850 MPa are bound to cause material failure.

Figure 13 displays the nature of strain profiles recorded from the loading of the component. Figure 13a reveals predominantly the elastic straining of the material with zero plastic strains while Figure 13b shows the magnitude of the elastic strains experienced at the edge of the component.

The results obtained show that the assigned Ti6Al4V material will be suitable for usage in the prescribed conditions for which these analyses were carried out. Furthermore, the material was found to have a great capacity to withstand the nature of forces and loads applied without failing since the resultant internal stresses, strains temperatures and displacements due to deformation fall within allowable ranges

4. CONCLUSION

This work considered the modelling and simulation of titanium alloy (Ti6Al4V) bearing housing of an aircraft manufactured additively. The excellent mechanical properties, such as high strength-to-weight ratio and good wear resistance, of the titanium alloy were explored. The design and the FEA were carried out using the Abaqus modelling and simulation tool. The design considerations include the suitability

for high speed and temperature application as well as high strength to support the load and absorb the induced stresses. The results obtained indicated that the designed bearing is suitable for high speed and temperature applications beyond 1900 K, which gives a strong indication of its ability to withstand such extreme conditions without melting, given the melting temperature of the material is about 1933 K. Using the Von Mises stress criterion, the maximum stress induced in the component during loading was 521 kPa. It is evident that the stresses developed do not result in a distortion or deformation of the material with yield strength being in the region of 820 MPa. This shows a good dimensional stability without any significant deformation or failure, which makes it suitable for aerospace applications. The value of the maximum stress induced at the inner ring of the bearing was significantly lower than the yield strength of the titanium alloy employed, thus indicating that the bearing is not likely to yield to failure under the required service conditions. This work provides design data for the development of bearing components using SLM because the values are in agreement to those published for laser-assisted machining and powder-based additive manufacturing for aerospace applications. This helps to detect the critical operating conditions early at the design stage before the fabrication of the bearing housing, in order to minimize any possible expensive reworks of the rig. This work did not consider the creep performance and dwell fatigue of the material (Ti6Al4V) at an elevated temperature, thus future works can consider the investigation of the potential for creep failure and dwell fatigue at high temperatures close to 1900 K.

ACKNOWLEDGEMENTS

Research support acknowledgements goes to the Department of Science and Technology in collaboration with the Council of Scientific and Industrial Research, (DST-CSIR), and the Research Chairs (Gibela) at the Industrial Engineering Department of Tshwane University of Technology Pretoria, all situated in South Africa.

REFERENCES

- [1] S. E. Haghighi, H. Lu, G. Jian, et al. Effect of α'' martensite on the microstructure and mechanical properties of beta-type Ti-Fe-Ta alloys. *Materials & Design* **76**:47–54, 2015. <https://doi.org/10.1016/j.matdes.2015.03.028>.
- [2] S. Ehtemam-Haghighi, Y. Liu, G. Cao, L.-C. Zhang. Influence of Nb on the $\beta \rightarrow \alpha''$ martensitic phase transformation and properties of the newly designed Ti-Fe-Nb alloys. *Materials Science and Engineering: C* **60**:503–510, 2016. <https://doi.org/10.1016/j.msec.2015.11.072>.
- [3] N. Taniguchi, S. Fujibayashi, M. Takemoto, et al. Effect of pore size on bone ingrowth into porous titanium implants fabricated by additive manufacturing: An in vivo experiment. *Materials Science and Engineering: C* **59**:690–701, 2016. <https://doi.org/10.1016/j.msec.2015.10.069>.
- [4] C. Bandapalli, B. M. Sutaria, D. V. Bhatt. High speed machining of Ti-alloys—A critical review. In *Proceedings of the 1st International and 16th National Conference on Machines and Mechanisms*, pp. 324–331. 2013.
- [5] W. Habrat, M. Motyka, K. Topolski, J. Sieniawski. Evaluation of the cutting force components and the surface roughness in the milling process of micro- and nanocrystalline titanium. *Archives of Metallurgy and Materials* **61**(3):1379–1384, 2016. <https://doi.org/10.1515/amm-2016-0226>.
- [6] E. Uhlmann, R. Kersting, T. B. Klein, et al. Additive manufacturing of titanium alloy for aircraft components. *Procedia CIRP* **35**:55–60, 2015. <https://doi.org/10.1016/j.procir.2015.08.061>.
- [7] G. Kasperovich, J. Hausmann. Improvement of fatigue resistance and ductility of TiAl6V4 processed by selective laser melting. *Journal of Materials Processing Technology* **220**:202–214, 2015. <https://doi.org/10.1016/j.jmatprotec.2015.01.025>.
- [8] L. Thijs, F. Verhaeghe, T. Craeghs, et al. A study of the microstructural evolution during selective laser melting of Ti-6Al-4V. *Acta Materialia* **58**(9):3303–3312, 2010. <https://doi.org/10.1016/j.actamat.2010.02.004>.
- [9] S. Leuders, M. Thöne, A. Riemer, et al. On the mechanical behaviour of titanium alloy TiAl6V4 manufactured by selective laser melting: Fatigue resistance and crack growth performance. *International Journal of Fatigue* **48**:300–307, 2013. <https://doi.org/10.1016/j.ijfatigue.2012.11.011>.
- [10] C. Y. Yap, C. K. Chua, Z. L. Dong, et al. Review of selective laser melting: Materials and applications. *Applied Physics Reviews* **2**(4):041101, 2015. <https://doi.org/10.1063/1.4935926>.
- [11] P. Michaleris. Modeling metal deposition in heat transfer analyses of additive manufacturing processes. *Finite Elements in Analysis and Design* **86**:51–60, 2014. <https://doi.org/10.1016/j.finel.2014.04.003>.
- [12] V. Vakharia, V. K. Gupta, P. K. Kankar. Nonlinear dynamic analysis of ball bearings due to varying number of balls and centrifugal force. In P. Pennacchi (ed.), *Proceedings of the 9th IFToMM International Conference on Rotor Dynamics*, pp. 1831–1840. Springer International Publishing, Cham, 2015. https://doi.org/10.1007/978-3-319-06590-8_151.
- [13] L. Zhu, N. Li, P. Childs. Light-weighting in aerospace component and system design. *Propulsion and Power Research* **7**(2):103–119, 2018. <https://doi.org/10.1016/j.jprr.2018.04.001>.
- [14] Z. Huda, P. Edi. Materials selection in design of structures and engines of supersonic aircrafts: A review. *Materials & Design* **46**:552–560, 2013. <https://doi.org/10.1016/j.matdes.2012.10.001>.
- [15] I. Inagaki, T. Takechi, Y. Shirai, N. Ariyasu. Application and features of titanium for the aerospace industry. *Nippon Steel and Sumitomo Metal Technical Report* **106**:22–27, 2014.
- [16] H. Clemens, S. Mayer. Design, processing, microstructure, properties, and applications of advanced intermetallic TiAl alloys. *Advanced Engineering Materials* **15**(4):191–215, 2013. <https://doi.org/10.1002/adem.201200231>.
- [17] C. Veiga, J. Davim, A. Loureiro. Properties and applications of titanium alloys: A brief review. *Reviews on Advanced Materials Science* **32**(2):133–148, 2012.
- [18] GE Additive. New manufacturing milestone: 30,000 additive fuel nozzles. [2019-01-09], <https://www.ge.com/additive/blog/new-manufacturing-milestone-30000-additive-fuel-nozzles>.
- [19] X. Wang, M. Jiang, Z. Zhou, et al. 3D printing of polymer matrix composites: A review and prospective. *Composites Part B: Engineering* **110**:442–458, 2017. <https://doi.org/10.1016/j.compositesb.2016.11.034>.
- [20] D. Bourell, J. P. Kruth, M. Leu, et al. Materials for additive manufacturing. *CIRP Annals* **66**(2):659–681, 2017. <https://doi.org/10.1016/j.cirp.2017.05.009>.
- [21] L. J. Kumar, C. G. Krishnadas Nair. *Current Trends of Additive Manufacturing in the Aerospace Industry*, pp. 39–54. Springer Singapore, Singapore, 2017. https://doi.org/10.1007/978-981-10-0812-2_4.
- [22] I. Daniyan, F. Fameso, K. Mpofu, I. D. Uchegbu. Modelling and simulation of surface roughness during the turning operation of titanium alloy (Ti6Al4V). In *2022 IEEE 13th International Conference on Mechanical and Intelligent Manufacturing Technologies (ICMIMT)*, pp. 176–181. 2022. <https://doi.org/10.1109/ICMIMT55556.2022.9845252>.
- [23] I. A. Daniyan, K. Mpofu, I. Tlhabadira, B. I. Ramatsetse. Process design for milling operation of titanium alloy (Ti6Al4V) using artificial neural network. *International Journal of Mechanical Engineering and Robotics Research* **10**(11):601–611, 2021. <https://doi.org/10.18178/ijmerr.10.11.601-611>.

- [24] I. A. Daniyan, I. Tlhabadira, K. Mpofu, R. Muvunzi. Numerical and experimental analysis of surface roughness during the milling operation of titanium alloy Ti6Al4V. *International Journal of Mechanical Engineering and Robotics Research* **10**(12):683–693, 2021. <https://doi.org/10.18178/ijmerr.10.12.683-693>.
- [25] S. Huang, R. L. Narayan, J. H. K. Tan, et al. Resolving the porosity-unmelted inclusion dilemma during in-situ alloying of Ti34Nb via laser powder bed fusion. *Acta Materialia* **204**:116522, 2021. <https://doi.org/10.1016/j.actamat.2020.116522>.
- [26] S. Huang, P. Kumar, W. Y. Yeong, et al. Fracture behavior of laser powder bed fusion fabricated Ti41Nb via in-situ alloying. *Acta Materialia* **225**:117593, 2022. <https://doi.org/10.1016/j.actamat.2021.117593>.
- [27] V. Chakkravarthy, M. Lakshmanan, P. Manojkumar, R. Prabhakaran. Crystallographic orientation and wear characteristics of TiN, SiC, Nb embedded Al7075 composite. *Materials Letters* **306**:130936, 2022. <https://doi.org/10.1016/j.matlet.2021.130936>.
- [28] U.S. Titanium Industry Inc. Titanium alloys – Ti6Al4V Grade 5. [2019-07-02], <https://www.azom.com/article.aspx?ArticleID=1547>.
- [29] S. Yang, Y. F. Zhao. Additive manufacturing-enabled design theory and methodology: a critical review. *The International Journal of Advanced Manufacturing Technology* **80**:327–342, 2015. <https://doi.org/10.1007/s00170-015-6994-5>.
- [30] J. Munguía, J. Lloveras, S. Llorens, T. Laoui. Development of an AI-based rapid manufacturing advice system. *International Journal of Production Research* **48**(8):2261–2278, 2010. <https://doi.org/10.1080/00207540802552675>.
- [31] M. Bici, S. Brischetto, F. Campana, et al. Development of a multifunctional panel for aerospace use through SLM additive manufacturing. *Procedia CIRP* **67**:215–220, 2018. <https://doi.org/10.1016/j.procir.2017.12.202>.
- [32] N. T. N. Matsumori. Bearings for jet engine main shafts to protect safety of aircrafts. *Tool Engineer* **54**(13):61, 2013.
- [33] A. Boschetto, L. Bottini, F. Veniali. Surface roughness and radiusing of Ti6Al4V selective laser melting-manufactured parts conditioned by barrel finishing. *The International Journal of Advanced Manufacturing Technology* **94**(5-8):2773–2790, 2018. <https://doi.org/10.1007/s00170-017-1059-6>.
- [34] I. A. Daniyan, F. Fameso, F. Ale, et al. Modelling, simulation and experimental validation of the milling operation of titanium alloy (Ti6Al4V). *The International Journal of Advanced Manufacturing Technology* **109**(7):1853–1866, 2020. <https://doi.org/10.1007/s00170-020-05714-y>.
- [35] I. Tlhabadira, I. Daniyan, L. Masu, K. Mpofu. Computer aided modelling and experimental validation for effective milling operation of titanium alloy (Ti6Al4V). *Procedia CIRP* **91**:113–120, 2020. <https://doi.org/10.1016/j.procir.2020.03.098>.
- [36] I. A. Daniyan, I. Tlhabadira, K. Mpofu, A. O. Adeodu. Development of numerical models for the prediction of temperature and surface roughness during the machining operation of titanium alloy (Ti6Al4V). *Acta Polytechnica* **60**(5):369–390, 2020. <https://doi.org/10.14311/AP.2020.60.0369>.
- [37] F. H. S. Froes. 1 - A historical perspective of titanium powder metallurgy. In M. Qian, F. H. (Sam) Froes (eds.), *Titanium Powder Metallurgy*, pp. 1–19. Butterworth-Heinemann, Boston, 2015. <https://doi.org/10.1016/B978-0-12-800054-0.00001-0>.
- [38] D. Wang, W. Dou, Y. Yang. Research on selective laser melting of Ti6Al4V: Surface morphologies, optimized processing zone, and ductility improvement mechanism. *Metals* **8**(7):471, 2018. <https://doi.org/10.3390/met8070471>.
- [39] B. Dutta, F. H. (Sam) Froes. 24 - The additive manufacturing (AM) of titanium alloys. In M. Qian, F. H. (Sam) Froes (eds.), *Titanium Powder Metallurgy*, pp. 447–468. Butterworth-Heinemann, Boston, 2015. <https://doi.org/10.1016/B978-0-12-800054-0.00024-1>.
- [40] T. Tulwin. A coupled numerical heat transfer in the transient multicycle CFD aircraft engine model. *Procedia Engineering* **157**:255–263, 2016. <https://doi.org/10.1016/j.proeng.2016.08.364>.
- [41] J. Krishnaraj, P. Vasanthakumar, J. Hariharan, et al. Combustion simulation and emission prediction of different combustion chamber geometries using finite element method. *Materials Today: Proceedings* **4**(8):7903–7910, 2017. <https://doi.org/10.1016/j.matpr.2017.07.126>.